JOURNAL OF OPTOELECTRONICS AND ADVANCED MATERIALS Vol. 19, No. 5 - 6, May – June 2017, p. 434 - 439

Structural, morphological and mechanical hardness properties of titanium nitride thin films deposited by DC magnetron sputtering: Effect of substrate temperature

M. T. HOSSEINNEJAD[a*], M. ETTEHADI-ABARI[a], N. PANAHI[b], M. A. FERDOSI ZADEH[c], S. W. CASE[b]
[a]Young Researchers and Elites Club, Science and Research Branch, Islamic Azad University, Tehran, Iran
[b]Department of Physics, Bandar Abbas Branch, Islamic Azad University, Bandar Abbas, Iran
[c]Department of Mechanical Engineering, Faculty of Engineering, Central Tehran Branch, Islamic Azad University, Tehran, Iran

Nano crystalline Titanium Nitride (TiN) thin films were deposited on glass substrates using DC reactive magnetron sputtering. The effect of substrate temperature on the structural, morphological and mechanical properties of TiN thin films has been investigated using different analysis. Obtained results from XRD analysis revealed that crystal structure characteristics of deposited thin films strongly depend on substrate temperature. According to the SEM and AFM results, the size of grains and surface roughness of deposited samples increased with increasing the temperature. Also hardness measurements revealed that the highest mechanical hardness is obtained when the film is deposited at 400°C substrate temperature.

(Received September 9, 2016; accepted June 7, 2017)

Keywords: TiN thin film, DC magnetron sputtering, Nanostructures, XRD, AFM

1. Introduction

Deposition of Titanium Nitride (TiN) film has widely introduced to various industrial coating fields such as hard, protective, high thermal stability, low electrical resistivity, high wear and excellent corrosion resistance [1,2], thermal stability [3] chemical stability [4] and biocompatibility [5]. Titanium nitride coatings have been widely applied as high temperature diffusion barrier for silicon devices in microelectronics, and wear resistant coatings in automobile [6-8]. The other areas of applications include high temperature photothermal conversion, biomedical materials and steel cutting tools [9]. Due to these special properties, TiN thin films have been deposited by a number of physical and chemical vapor deposition methods including evaporation, ion plating and sputtering [10–14].

In order to deposit the thin film on any substrate, it is common to use processes such as physical vapor deposition (PVD) [15,16], plasma enhanced chemical vapor deposition (PECVD) [17], plasma assisted chemical vapor deposition (PACVD) and plasma focus (PF) method [18,19]. Among those processes, DC sputtering process is known to be easy and to present a good adhesion between the film and the substrates of metals and ceramics. DC Magnetron Sputtering (DCMS) has occupied the attention of the related researchers due to its wide range of applications. In this method, the properties of deposited thin films, like preferred orientation of lattice plane, grown by physical and chemical vapor deposition methods are highly dependent on total gas pressure, partial pressures of reactive gases, deposition rate, substrate temperature, flux of bombarding particles and substrate material [20–27]. The mentioned parameters are known to influence grain growth and crystallographic texture, which affect the resulting microstructure and properties of the films. This makes it suitable for a wide range of applications if the material properties are tuned right.

Several studies about structural, mechanical and electrical properties of TiN thin films have been completed in the last years [28-30]. For example photoacoustic measurement of the thermal properties of the films revealed that the thermal diffusivity and thermal conductivity of the TiN thin films are significantly lower than the bulk values and that the grain size of the films has substantial influence on the thermal properties of TiN thin films.

Thermal property data are important for any material that experiences heat transfer. Knowledge of thermal diffusivity and thermal conductivity of TiN thin films is essential for their long-term use in devices and for understanding the thermal aging effects and deterioration of films in the area of microelectronics and tribology, where TiN films are used in one form or another [9]. Though the thermal property data of TiN coatings are important from the fundamental and technical point of view, little work [24] has been done on measuring this quantity.

In which the film is deposited on glass substrate using the DC magnetron sputtering process as a function of substrate temperature at the constant Ar : N_2 gas ratio. In this investigation, various characteristics of the deposited

films, relevant to their structure, surface morphology and hardness, are reported for various conditions of deposition in terms of substrate temperature.

2. Experimental details

The TiN films were prepared by sputtering a 99.999% pure Ti disc of 5.5 cm diameter and 0.5 mm thickness in a mixture of high purity argon and nitrogen plasma. The base pressure was 5×10^{-5} Torr and the sputtering was carried out in Ar : N_2 (70% : 30%) under pressure of 5×10^{-2} Torr. The sputtering was carried out in a Pyrex chamber of 15 cm diameter and 10 cm depth using DC magnetron sputtering. The glass substrates used for deposition of the films were of same dimension (10 mm, 10 mm) and were ultrasonically cleaned in acetone for 15 min and dried by blowing hot air before being placed in the vacuum chamber. Schematic view of DC magnetron sputtering system is show in Fig. 1.

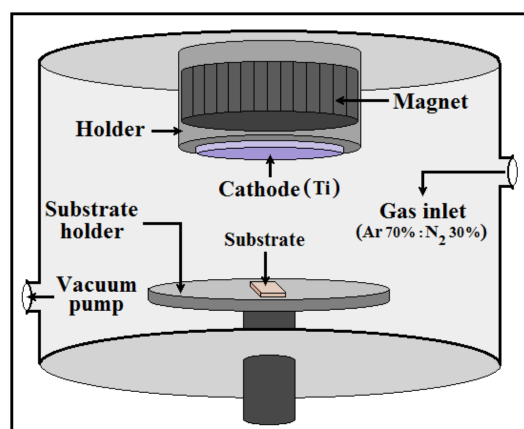

Fig. 1. Schematic view of the low pressure DC magnetron sputtering system

During all depositions the target-to-substrate distance and sputtering power were kept fixed at 50 mm and 15 W, respectively. TiN films were deposited at different substrate temperatures (100 °C, 200 °C, 300 °C and 400 °C). High purity argon and nitrogen was fed into the vacuum chamber for the plasma generation and the substrates were treated for 60 min.

In magnetron sputtering the deposition parameters such as substrate temperature, pressure, and sputtering power influence directly on thin film parameters such as grain growth, morphology and so on. Since the substrate temperature is an effective factor on forming a uniform thin film, we applied different substrate temperatures and investigated structural, morphological and mechanical properties of deposited samples.

Generally two processes occur on the glass surface during film deposition: nitrogen ions accelerate towards the glass substrate and deliver energy instantly, causing high thermal gradients. Consequently, high heating and cooling rates are developed into surface layer of glass. Nitrogen ions cause etching and cleaning the substrate surface prior to deposition. On the other hand, electrons accelerate towards the titanium cathode, and ablate the material from cathode. The ablated material can interact with reactive nitrogen ions to form titanium nitride and deposit at glass substrate. The nitrogen ions can also react with these deposited titanium atoms, resulting in greater TiN content in the film.

Deposition conditions and coating results for runs are summarized in Table 1.

Table 1. Sputtering conditions of TiN thin films

Objects	***Specification***
Target	Ti (99.999%)
Substrate	Glass
Target-substrate distance	50 mm
Base pressure of chamber	5×10^{-5} Torr
Working pressure	5×10^{-2} Torr
System power	15 W
Sputtering gas (Ar: N_2)	70:30
Substrate temperature	100, 200, 300, 400 °C

In this work, the deposited TiN films were characterized for their structure, surface morphology and mechanical properties by different techniques. Crystalline structure of the thin films were studied using a STOE model STADI MP Diffractometer, (CuK_α radiation) with a step size of 0.01° and count time of 1.0 second per step. Surface morphology of thin films were investigated using Scanning Electron Microscopy (SEM, LEO 440i) and Atomic Force Microscopy (AFM, Auto Probe Pc; in contact mode, with low stress silicon nitride tip of less than 200 °A radius and tip opening of 18°). Average thickness of the deposited samples was measured with surface profiler with the accuracy of 10 nm (Dektak 3030, Veeco instruments Inc.) Moreover, the hardness measurements were performed using Nanoindenter (Fisher scope, H100C).

3. Results and discussion

The structural properties of the TiN thin films deposited at different substrate temperatures were investigated by XRD analysis. XRD measurements were made using CuK_α radiation to characterize the TiN thin films. The scan rate used was 1°/min and the scan range was from 20° to 60°. XRD patterns of the deposited samples are presented in Fig. 2.

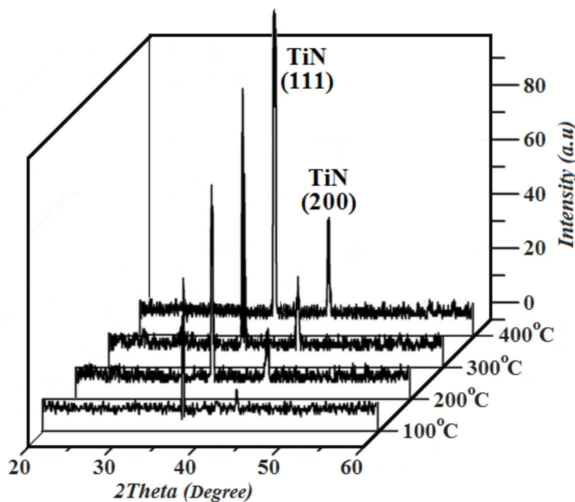

Fig. 2. XRD patterns of TiN thin films deposited at various substrate temperatures

The respective positions of the diffraction peaks are in agreement with joint committee for powder diffraction standards (JCPDS) standard data for TiN powders (refer to JCPDS card No. 00-038-1420). These patterns evidence emergence of TiN crystalline phase on glass substrates for all samples deposited at various substrate temperatures.

Fig. 3a reveals variations of the relative intensities of TiN (111) and TiN (200) diffraction peaks as a function of substrate temperatures. From Fig. 3*a*, it is observable that the degree of crystallinity of the deposited thin films depends on the substrate temperatures. Indeed, the degree of crystallinity of the TiN deposited samples, for all crystalline planes, increases by increasing the substrate temperature. The increase in relative intensity of the TiN peaks can be attributed to increasing thickness of the crystalline nitride phase material with the increasing the substrate temperature which will result in increase in diffracted photon counts if X-Ray can still penetrate up to the increased depth of titanium nitride crystalline layer.

The crystal size of the thin films was estimated from the Scherrer formula, as given in Eq. (1). In this expression, the crystal size D is along the surface normal direction, which is also the direction of the XRD diffraction vector.

$$D = K\lambda / (\beta \cos\theta) \qquad (1)$$

where D is the crystal size, K is a Scherer constant (usually 0.9), λ is the wavelength (15.405 nm for CuK_{α}), and θ is the Bragg angle. Also in this equation β is obtained from the equation $\beta^2 = \beta_r^2 - \beta^2_{strain} - C^2$, where $\beta_{strain} = \varepsilon \tan(\theta)$ is the lattice broadening from the residual strain ε measured by XRD using the $\cos 2\alpha \cos 2\psi$ method, β_r is the corrected full-width at half maximum (FWHM), and C is the instrumental line broadening [31]. Fig. 3b shows the variation of average crystal size calculated by Scherrer formula, for different deposited samples. Obtained results reveal an increase in crystal size with increasing the temperature, which indicates an improvement in the crystalline nature of the coatings [32]. In other words, this result suggests that the substrate temperature has strong effects on the lattice constant of TiN grown in Ar : N_2 mixed gas. As the substrate temperature increases, there is an increase in the adatom mobility of the sputtered species on the substrate. This causes an increasing crystal size with increasing substrate temperature.

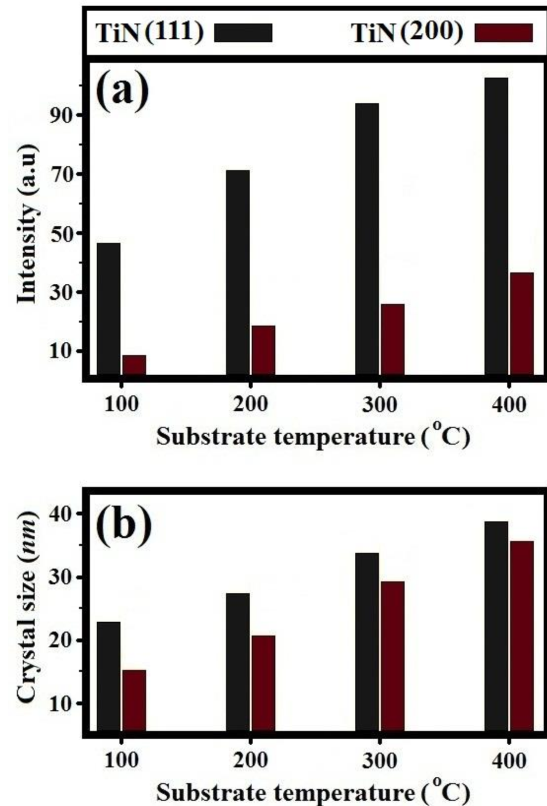

Fig. 3. Variation of (a) relative peak intensity and (b) crystallite size estimated from TiN (1 1 1) and TiN (2 0 0) planes as a function of substrate temperature.

Fig. 4 shows the SEM micrographs of TiN thin films deposited at the different substrate temperatures. The SEM micrographs of TiN films reveal the growth of TiN structures by increasing the temperature. The results clearly demonstrate that the thermal properties of the substrates have substantial influence on the growth of TiN thin films. Increasing temperature leads to the more mobility of the sputtered species on the substrate which this causes an increasing grain growth with increasing substrate temperature.

Moreover, the morphology of TiN thin films deposited is in accordance with the structural zone models discussed by J.A. Thornton [33]. Titanium nitride has a high melting temperature T_m = 2930 °C. At this temperature, T_s/T_m is less than 0.17 allowing only zone 1 structure, where T_s is the substrate temperature and T_m is the melting point of the film.

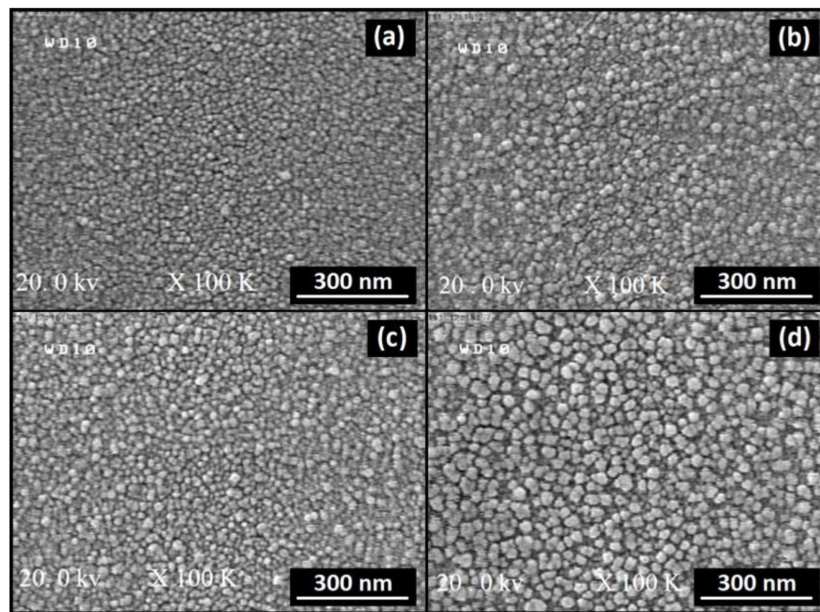

Fig. 4. The SEM images of deposited samples at
(a) 100 °C, (b) 200 °C, (c) 300 °C and (d) 400 °C substrate temperatures

Using AFM, we have analyzed the surface morphology of the films deposited at various substrate temperatures. The 3D surface topography of the deposited thin films is shown in Fig. 5. In this investigation, atomic force microscope is used in contact mode and all images have been obtained in a scanning area of 1 μm x 1 μm.

From AFM images it is observable that with increasing the substrate temperature, distributions of the grains on the sample surfaces are more heterogeneous with a low distribution of sparse clusters. Same possible explanation applies here: Increasing temperature leads to the more mobility of the sputtered species on the substrate which this causes an increasing grain growth with increasing substrate temperature.

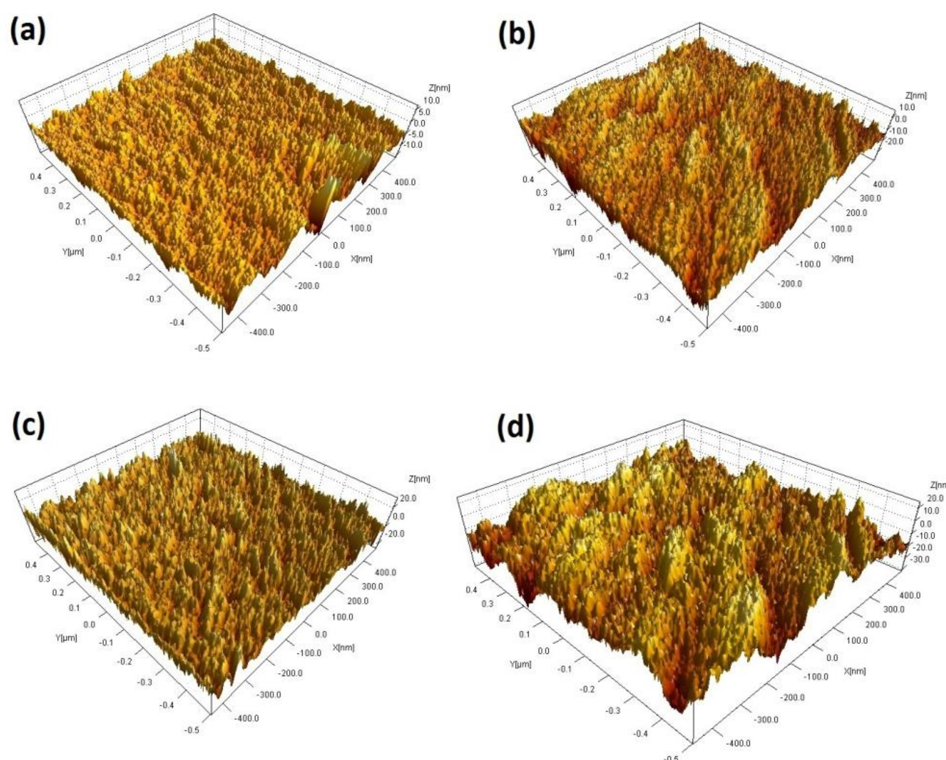

Fig. 5. The AFM images of deposited samples at
(a) 100 °C, (b) 200 °C, (c) 300 °C and (d) 400 °C substrate temperatures

Also the values of average and root mean square (RMS) surface roughness are derived from AFM images. Since surface roughness may slightly vary on different points of surface, to achieve more accurate results, we have measured it on three different points and reported the average in the paper. The recorded average and RMS values of the roughness measurements are plotted versus the substrate temperature and shown in Fig. 6.

Results indicate that average and RMS roughness of deposited samples increase by increasing the temperature. This is predictable because with increasing the temperature, the size of the grains becomes larger on the surface of the films which will lead to increasing the roughness of the deposited samples.

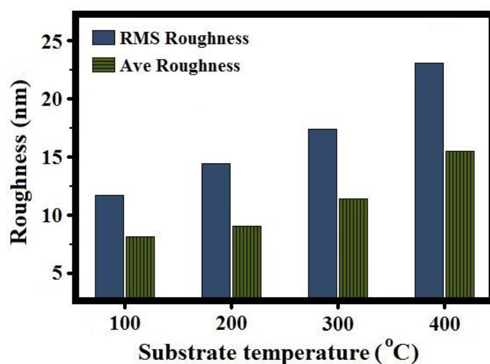

Fig. 6. Variations of the RMS and average roughness of the film surface in terms of the substrate temperature

Average thickness of the samples was measured with surface profiler with the accuracy of 10 nm (Dektak 3030, Veeco instruments Inc.). The Average thickness of the deposited thin films is presented in Table 2.

Table 2. The average thickness of TiN samples deposited with different Substrate temperatures

Substrate temperature (°C)	100	200	300	400
Average thickness (nm)	70	140	170	260

Thickness measurements show the increasing of average thickness of the deposited thin films when the substrate temperature increases from 100 °C to 400 °C. As it was mentioned earlier, increasing the substrate temperature leads to increasing the crystal size of deposited thin films. Therefore, the thickness of deposited samples increases with increasing the substrate temperature. Also as it can be seen from SEM images, the size of grains increases with substrate temperature, hence the average thickness of thin films increase with increasing the temperature. On the other hand, as it was mentioned earlier, the increasing of diffraction peaks intensities of deposited samples with increasing the substrate temperature also confirms that the thickness of TiN thin film increases with increasing the substrate temperature.

In order to assess the mechanical properties of the coated TiN thin films, nanoindentation measurements were taken. Fig. 7 shows the hardness and Young's modulus of the deposited samples at different substrate temperatures that were determined from 50 nm to 60 nm penetration depth. This indentation depth was selected to cause adequate plastic deformation during indentation but to avoid the substrate effect [34].Three measurements are performed at different locations to account the average values of hardness for each deposited sample.

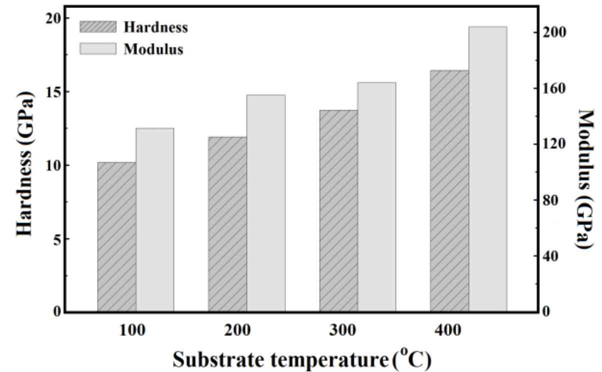

Fig. 7. Hardness and Young's modulus of prepared TiN thin films in terms of the substrate temperature

From Fig. 7 it is observable that the hardness of the deposited samples increases when the substrate temperature increases from 100 °C to 400 °C. These results could also be speculated from the XRD patterns shown in Fig. 2 which shows the crystalline phase of the titanium nitride increasing with increasing the substrate temperature. This change in degree of crystallinity of deposited samples along with the increase in the thickness of the thin films with the increase in substrate temperature can be responsible for increase in the hardness of the deposited thin films.

4. Conclusions

A systematic study has been performed to investigate the effect of the substrate temperature in the DC sputtering, on the growth behavior of TiN phase on glass substrate. The TiN thin films were successfully prepared by reactive DC magnetron sputtering in the gaseous mixture of Ar (70%) and N_2 (30%).

The XRD results suggested that the degree of crystallinity of the TiN deposited thin film and also the average crystallite sizes of the diffraction peaks for the TiN (1 1 1) and TiN (2 0 0) crystalline planes increase by increasing the substrate temperature. SEM analysis revealed the growth of TiN structures by increasing the temperature. These images indicated that the size of grains increase with increasing the substrate temperature. From AFM analysis observed that the size of grains and surface roughness of the thin films constantly increase with increasing the substrate temperature. Also obtained results from hardness analysis presented that hardness of deposited samples increases with increasing the substrate

temperature which were in agreement with XRD results. Thus, the results clearly demonstrate that the structural, morphological and mechanical properties of deposited thin films have substantial influence on the thermal properties of TiN thin films.

References

[1] K. Feng, Z. Li, F. Lu, J. Huang, X. Cai, Y. Wu, J. Power Sources **249,** 299 (2014).
[2] M. Tacikowski, M. Banaszek, J. Smolik, Vacuum **99,** 298 (2014).
[3] J. L. Schroeder, B. Saha, M. Garbrecht, N. Schell, T. D. Sands, J. Birch, J. Mater. Sci. **50,** 3200 (2015).
[4] J. F. Marco, J. R. Gancedo, M. A. Auger, O. Sánchez, J. M. Albella, Surf. Interface Anal. **37,** 1082 (2005).
[5] L. Duta, G. E. Stan, A. C. Popa, M. A. Husanu, Materials **9,** 38 (2016).
[6] S. Veprek, M.J.G. Veprek-Heijman, Surf. Coat. Technol. **202**, 5063 (2008).
[7] S. Kanamori, Thin Solid Films **136,** 195 (1986).
[8] K. Hinode, Y. Homma, M. Horiuchi, T. Takhashi, J. Vac. Sci. Technol. A **15,** 2017 (1997).
[9] A. Albert Irudayaraj, R. Srinivasan, P. Kuppusami, E. Mohandas, S. Kalainathan. K. Ramachandran, J. Mater. Sci. **43,** 1114 (2008).
[10] N. K. Ponon, D. J. R. Appleby, E. Arac, P. J. King, S. Ganti, K.S.K. Kwa, A. O'Neill, Thin Solid Films **578,** 31 (2015).
[11] S. Talu, S. Stach, S. Valedbagi, S. M. Elahi, R. Bavadi, Materials Science-Poland **33,** 137 (2015).
[12] R. Alipour, A. A. Khani, R. Mohammadi, S. Rostami, J. Chem. Research **40,** 12 (2016).
[13] K. H. Thulasi Raman, T. R. Penki, N. Munichandraiah, G. Mohan Rao, Electrochimica Acta **125**, 282 (2014).
[14] N. White, A. L. Campbell, J. T. Grant, R. Pachter, K. Eyink, R. Jakubiak, G. Martinez, C. V. Ramana, Applied Surface Science **292,** 74 (2014).
[15] E. Zalnezhad, A. A. D. Sarhan, M. Hamdi, Int. J. Adv. Manuf. Technol. **64,** 281 (2013).
[16] B. Tian, W. Yue, Z. Fu, Y. Gu, C. Wang, J. Liu, Vacuum **99,** 68 (2014).
[17] J. Lee, J. H. Jeon, C. H. Je, Y. G. Kim, S. Q. Lee, W. S. Yang, J. S. Lee, S. G. Lee, J. Micromechanics and Microengineering **25,** 125022 (2015).
[18] M. T. Hosseinnejad, M. Shirazi, Z. Ghorannevis, M. Ghoranneviss, F. Shahgoli, J. Fusion Energy **31,** 426 (2012).
[19] M. T. Hosseinnejad, M. Shirazi, M. Ghoranneviss, M. R. Hantehzadeh, Ceramics International **41,** 15024 (2015).
[20] P. P. Sahay, R. K. Nath, S. Tewari, Crystal Res. Technol. **42,** 275 (2007).
[21] P. P. Sahay, R. K. Mishra, S. N. Pandey, S. Jha, M. Shamsuddin, Current Applied Physics **13,** 479 (2013).
[22] M. Shirazi, M. T. Hosseinnejad, A. Zendehnam, M. Ghoranneviss, G. R, Etaati, J. Alloys and Compounds **602,** 108 (2014).
[23] K. Zhu, Y. Yang, W. Song. Materials Letters **145**, 279 (2015).
[24] F. Vaz, J. Ferreira, E. Ribeiro, L. Rebouta, S. Lanceros-Mendez, J. A. Mendes, E. Alves, Surf. Coat. Technol. **191,** 317 (2005).
[25] M. T. Hosseinnejad, M. Shirazi, M. Ghoranneviss, M. R. Hantehzadeh, E. Darabi, J. Inorg. Organomet. Polym. Mater. **26,** 405 (2016).
[26] N. Panahi, M. T. Hosseinnejad, M. Shirazi, M. Ghoranneviss, Chin. Phys. Lett. **33,** 066802 (2016).
[27] M. Shirazi, M. T. Hosseinnejad, A. Zendehnam, Z. Ghorannevis, Applied Surface Science **257,** 10233 (2011).
[28] J. Crummenauer, H. R. Stock, P. Mayr, Mater. Manuf. Processes, **10,** 1267 (1995).
[29] M. Popovic, M. Novakovic, N. Bibic, Mater. Character. **60,** 1463 (2009).
[30] M. Omrani, M. Habibi, R. Amrollahi, A. Khosravi, Int. J. Hydrogen Energy **37,** 14676 (2012).
[31] B. E. Warren, J. Biscoe, J. Am. Ceram. Soc. **21,** 49 (1938).
[32] B. Subramanian, R. Ananthakumar, M. Jayachandran, Surf. Coat. Technol. **205,** 3485 (2011).
[33] J. A. Thornton, Ann. Rev. Mater. Sci. **7,** 239 (1977).
[34] L. Y. Lin, M. C. Jeong, D. E. Kim, J. M. Myoung, Surf. Coat. Technol. **201,** 2547 (2006).

*Corresponding author: hoseinnejad.pprc@gmail.com